



# Transcriptome Profiling of Tomato Uncovers an Involvement of Cytochrome P450s and Peroxidases in Stigma Color Formation

Yan Zhang<sup>1,2</sup>, Guiye Zhao<sup>1,2</sup>, Yushun Li<sup>1,2</sup>, Jie Zhang<sup>1,2</sup>, Meijing Shi<sup>1,2</sup>, Tayeb Muhammad<sup>1,2</sup> and Yan Liang<sup>1,2\*</sup>

<sup>1</sup> College of Horticulture, Northwest A&F University, Yangling, China, <sup>2</sup> State Key Laboratory of Crop Stress Biology in Arid Region, Northwest A&F University, Yangling, China

## OPEN ACCESS

### Edited by:

Stefan de Folter,  
Centro de Investigación y de Estudios  
Avanzados del Instituto Politécnico  
Nacional, Mexico

### Reviewed by:

Concepción Gómez-Mena,  
Instituto de Biología Molecular y  
Celular de Plantas (CSIC), Spain  
Vagner Benedito,  
West Virginia University, United States

### \*Correspondence:

Yan Liang  
liangyan@nwsuaf.edu.cn

### Specialty section:

This article was submitted to  
Plant Evolution and Development,  
a section of the journal  
Frontiers in Plant Science

**Received:** 13 April 2017

**Accepted:** 12 May 2017

**Published:** 31 May 2017

### Citation:

Zhang Y, Zhao G, Li Y, Zhang J,  
Shi M, Muhammad T and Liang Y  
(2017) Transcriptome Profiling  
of Tomato Uncovers an Involvement  
of Cytochrome P450s  
and Peroxidases in Stigma Color  
Formation. *Front. Plant Sci.* 8:897.  
doi: 10.3389/fpls.2017.00897

Stigma is a crucial structure of female reproductive organ in plants. Stigma color is usually regarded as an important trait in variety identification in some species, but the molecular mechanism of stigma color formation remains elusive. Here, we characterized a tomato mutant, *yellow stigma* (*ys*), that shows yellow rather than typical green color in the stigma. Analysis of pigment contents revealed that the level of flavonoid naringenin chalcone was increased in the *ys* stigma, possibly as a result of higher accumulation of *p*-coumaric acid, suggesting that naringenin chalcone might play a vital role in yellow color control in tomato stigma. To understand the genes and gene networks that regulate tomato stigma color, RNA-sequencing (RNA-Seq) analyses were performed to compare the transcriptomes of stigmas between *ys* mutant and wild-type (WT). We obtained 507 differentially expressed genes, in which, 84 and 423 genes were significantly up-regulated and down-regulated in the *ys* mutant, respectively. Two cytochrome P450 genes, *SIC3H1* and *SIC3H2* which encode *p*-coumarate 3-hydroxylases, and six peroxidase genes were identified to be dramatically inhibited in the yellow stigma. Further bioinformatic and biochemical analyses implied that the repression of the two *SIC3Hs* and six *PODs* may indirectly lead to higher naringenin chalcone level through inhibiting lignin biosynthesis, thereby contributing to yellow coloration in tomato stigma. Thus, our data suggest that two *SIC3Hs* and six *PODs* are involved in yellow stigma formation. This study provides valuable information for dissecting the molecular mechanism of stigma color control in tomato.

**Statement:** This study reveals that two cytochrome P450s (*SIC3H1* and *SIC3H2*) and six peroxidases potentially regulate the yellow stigma formation by indirectly enhancing biosynthesis of yellow-colored naringenin chalcone in the stigma of tomato.

**Keywords:** cytochrome P450s, peroxidases, tomato, transcriptome, yellow stigma

## INTRODUCTION

Pollination is a crucial event in sexual reproduction that sustains lifecycle of flowering plants on the face of the earth. The stigma, which functions as the recipient of pollen, shows wide variation in colors similar to flowers. Different colors of flowers and those of stigmas are attributed to accumulation of diverse pigments, which may attract specific pollinators to facilitate pollination. For example, in some species, such as *Arabidopsis* and tomato (*Solanum lycopersicum*), the color of stigma is green, whereas that in cucumber (*Cucumis sativus* L.) is yellow. Furthermore, the stigma color is often regarded as an important trait in variety identification in some crop plants such as rice (*Oryza sativa*). For instance, in many rice cultivars of Asia, the stigmas are colorless, but in most of wild germplasms, those are colored, signifying their involvement in the process of domestication (Han et al., 2006). So far, extensive studies have confirmed that the flower colors are due mainly to flavonoids, carotenoids and betalains, in which, the flavonoids are the most crucial (Grotewold, 2006; Tanaka and Brugliera, 2013; Gao et al., 2016). However, little is known about the involvement of pigments, especially flavonoids, in the formation of color in the stigma.

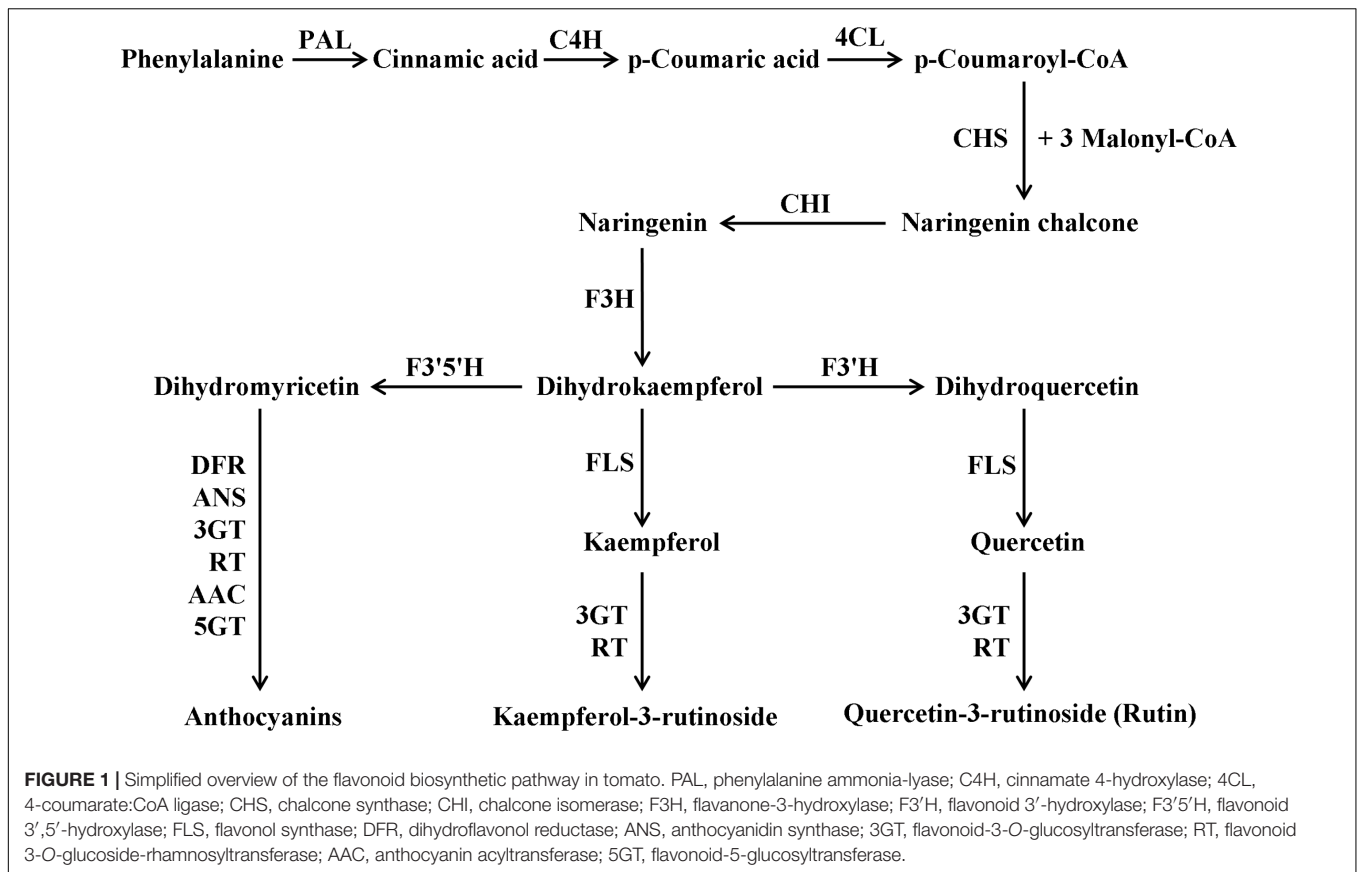
Flavonoids, a large group of plant polyphenols, are widely distributed throughout the plant kingdom. Until now, over 10,000 structures of flavonoids have been identified in plants (Julkunen-Tiitto et al., 2015). This diversity arises from combinatorial modifications of the basic flavonoid scaffold by decorating enzymes such as glycosyl, acyl, and methyl transferases, and also due to structural differences in the basic flavonoid skeleton such as isoflavonoids (Mehrtens et al., 2005). In addition to their functions as floral pigments, flavonoids play important roles in many other aspects of plant growth, development and responses to environmental stimuli, such as regulation of auxin transport, male fertility, pollination, pathogen resistance, and UV-light protection (Harborne and Williams, 2000; Zhang et al., 2015). Furthermore, flavonoids are good antioxidants and have been demonstrated to promote human health and reduce the primary risk factor for some diseases when consumed as foods from plant origin (Hannum, 2004; Hooper and Cassidy, 2006; Tapas et al., 2008; Martin et al., 2011; Li et al., 2015). Flavonoids can be classified into different subgroups: chalcones, flavones, flavonols, flavanones, isoflavones, flavanols, and anthocyanins, in which, the chalcones function as yellow pigments in many flowers, the anthocyanins usually display

red, purple, and blue colors, while several other classes such as flavonols and flavanols serve as co-pigments (Tanaka et al., 2008; Petrusa et al., 2013).

The flavonoid biosynthetic pathway has been well established (Figure 1), and it is conserved among seed plants (Tanaka et al., 2008; Buer et al., 2010; Petrusa et al., 2013; Saito et al., 2013; Weston and Mathesius, 2013). Flavonoids are biosynthesized along the general phenylpropanoid pathway in the cytosol (Winkel, 2004). Previous studies have shown that the enzymes involved in the biosynthetic pathway form a multienzyme complex (metabolon) via protein-protein interaction and bind to the ER membrane (Grotewold, 2006; Ono et al., 2006; Kuhn et al., 2011). These enzymes belong to several enzyme families, such as cytochrome-P450, OGD, and GT (Tanaka, 2006; Tanaka et al., 2008). The genes encoding these biosynthetic enzymes of the pathway, such as *CHS*, *CHI*, *F3'H*, *F3'5'H*, *FLS*, *DFR*, *ANS*, *3GT*, flavonoid 3-O-glucosyltransferase (*RT*) and *5GT* have been cloned and analyzed in different plant species (Shirley et al., 1995; Pourcel et al., 2005; Buer et al., 2007; Owens et al., 2008a,b; Buer and Djordjevic, 2009; Falcone Ferreyra et al., 2015). Besides these biosynthetic genes, combinations of the R2R3-MYB, bHLH and WDR factors and their interactions are also involved in regulation of flavonoid biosynthesis at the transcriptional level. This model has been well understood in *Arabidopsis*, tomato, maize (*Zea mays*) petunia (*Petunia hybrida*) and some other plants (Koes et al., 2005; Ramsay and Glover, 2005; Morita et al., 2006; Gonzali et al., 2009; Xu et al., 2015). MYB and bHLH transcription factors (TFs) are the largest families among plant TFs and are found in all eukaryotes (Heim et al., 2003; Dubos et al., 2010; Feller et al., 2011), whereas WDR proteins are pleiotropic, which participate in multiple processes such as flavonoid biosynthesis, the fate of multiple epidermal cells and the formation of trichomes and root hairs (Tanaka et al., 2008; Li et al., 2014). Interestingly, these three proteins can form a ternary complex named as MBW (MYB-bHLH-WDR) (Baudry et al., 2004). It is believed that the MBW complex is directly responsible for the activation of flavonoid LBGs expression (Gonzalez et al., 2008; Thevenin et al., 2012; Xu et al., 2014, 2015).

Tomato has been widely cultivated as an important vegetable crop around the world. Although the flavonoid biosynthetic pathway is well established in tomato (Ye et al., 2015), the majority of the studies are focused on flavonoids-regulated color formation in tomato fruits. Until now, around 70 flavonoids have been identified in tomato fruit, which are predominantly accumulated in the fruit peel (Bovy et al., 2002; Colliver et al., 2002; Iijima et al., 2008; Ballester et al., 2010). The major flavonoids in tomato fruit are naringenin chalcone, quercetin, kaempferol, and their conjugated forms such as different glycosides (Moco et al., 2006). Among them, yellow-colored naringenin chalcone, one of the most abundant flavonoids in tomato fruit, is accumulated in the cuticle during the fruit ripening and thus determines the yellow color in the peel at the breaker stage. In addition, quercetin-3-rutinoside (rutin) and kaempferol-3-rutinoside are also distributed in the peel of ripen fruit (Ballester et al., 2010).

**Abbreviations:** ANS, anthocyanidin synthase; bHLH, basic helix-loop-helix; C3H, *p*-coumarate 3-hydroxylase; CHI, chalcone isomerase; CHS, chalcone synthase; DEG, differentially expressed gene; DFR, dihydroflavonol reductase; DGE, differentially gene expression; EMS, ethylmethane sulfonate; ER, endoplasmic reticulum; FDR, false discovery rate; F3'H, flavonoid 3'-hydroxylase; F3'5'H, flavonoid 3',5'-hydroxylase; FLS, flavonol synthase; FPKM, fragments per kilobase of exon per million mapped fragments; FSII, flavone synthase II; GO, Gene Ontology; GT, glucosyltransferases; 3GT, flavonoid-3-O-glucosyltransferase; 5GT, flavonoid-5-glucosyltransferase; HPLC, high performance liquid chromatography; KEGG, Kyoto Encyclopedia of Genes and Genomes; LBGs, late biosynthetic genes in flavonoid biosynthetic pathway; LC-MS, liquid chromatograph-mass spectrometer; OGD, 2-oxoglutarate-dependent dioxygenases; PDA, photo-diode array; POD, peroxidase; qRT-PCR, quantitative real-time PCR; RT, flavonoid 3-O-glucoside-rhamnosyltransferase; WDR, WD40-repeat; WT, wild-type; *ys*, yellow stigma.



Despite the importance of the stigma as an essential structure of female reproductive organ, little is known about the mechanism of the regulation of stigma color in plants. Moreover, to the best of our knowledge, there are no identified tomato mutants with different colors of stigmas. In this study, through EMS mutagenesis, we identified a mutant with unusual yellow stigma color. This mutant was named as *ys*. We investigated the pigment contents in the stigmas of *ys* mutant and WT (green stigma), and performed comparative transcriptome profiling analyses to elucidate genes and gene networks involved in yellow stigma formation in tomato. Our study revealed that the accumulation of yellow-colored flavonoid naringenin chalcone was significantly increased in the yellow stigma, and two cytochrome P450 genes, *SIC3H1* and *SIC3H2* that encode the *p*-coumarate 3-hydroxylases, and six POD genes might participate in yellow stigma formation through indirect regulation of the naringenin chalcone level in the *ys* mutant. These results provide valuable information for dissecting the molecular mechanism of yellow stigma formation in tomato.

## MATERIALS AND METHODS

### Plant Materials and Growth Conditions

The *ys* mutant of tomato was generated in the background of the inbred line TTD302A through EMS mutagenesis using Saito's method (Saito et al., 2011), and stabilized via six generations of

selfing prior to this study. The seeds of *ys* mutant and WT were germinated on wet filter paper in a Petri dish at 28°C in dark for 3 days. Then the resulting seedlings were grown in a growth chamber under a 16 h/8 h (light/dark) photoperiod with 25/16°C temperatures, respectively. Upon four true-leaf stage, plants were transferred to a greenhouse in the experimental field of the Northwest A&F University. Pest control and water management were carried out according to standard practices.

### Measurement of Chlorophyll, Carotenoid, and Flavonoid Levels

The fresh stigmas at the anthesis stage were collected from WT and *ys* mutant at the same time on the same day, and then immediately used to pigment measurement. Total chlorophylls and carotenoids were extracted and quantified by spectrophotometric method as described previously (Lichtenthaler, 1987; Bou-Torrent et al., 2015).

Flavonoids and other polyphenols extraction and analyses were carried out according to Bino et al. (2005) with some modifications. The 100 mg frozen tomato stigmas powder was extracted with 80% methanol for 12 h at 4°C followed by 30 min sonication. The mixtures were then centrifuged at 12,000 rpm for 10 min at 4°C and the supernatants were filtered (0.2 μm). The extraction was repeated once by the above method. The samples were analyzed and identified using a Waters Alliance 2695 HT HPLC system coupled with a Q-TOF Mass Spectrometer

(Waters-Micromass, Milford, MA, United States). The 20  $\mu\text{L}$  of sample extract was injected and separated using a Luna C18 reverse-phase analytical column (3  $\mu\text{m}$ , 150 mm  $\times$  2.1 mm; Phenomenex) at 40°C and a gradient of 5–50% acetonitrile in 0.1% formic acid at a flow rate of 0.3 mL  $\text{min}^{-1}$ . The eluted compounds were detected at 200–600 nm using a 996 PDA detector (Waters, Milford, MA, United States), followed by the mass spectrometer equipped with an electrospray ionization (ESI) source. The conditions for LC-MS runs were as follows: desolvation temperature was 250°C with a nitrogen gas flow rate of 10 L  $\text{min}^{-1}$  and capillary voltage was 3 kV; source temperature was 120°C; cone voltage was 35 eV with 1 L  $\text{min}^{-1}$  gas flow and collision energy was 5 eV in positive ion mode or 10 eV in ion mode. Ions in the  $m/z$  range 100–1500 were detected using a scan time of 0.9 s and an interscan delay of 0.1 s. The flavonoid compounds and other polyphenols were identified using retention times obtained by authentic standards and mass calculated for the ion ( $M + H$ )<sup>+</sup> (Supplementary Table S1), and quantified by comparing the area of each individual peak with the standard curves obtained from the pure compounds. All measurements were repeated with three independent biological samples, and each sample was assayed in triplicate.

### Lignin Content Determination

The stigmas at the anthesis stage from WT and *ys* mutant were harvested and freeze-dried in liquid nitrogen. The lignin content was determined using the acetyl bromide method as described previously with some modifications (Yan et al., 2012). The samples were ground into powder, then 10 mg of powder was rinsed four times with 95% ethanol and twice with the mixture of 100% ethanol and *n*-hexane (1:2 in volume). The precipitate was collected, dried at 60°C and then suspended in 2 mL of 25% acetyl bromide in glacial acetic acid. After incubation at 70°C for 30 min, 0.9 mL 2 M NaOH was added, followed by 2 mL glacial acetic acid and 0.1 mL 7.5 M hydroxylamine hydrochloride. The mixture was centrifuged at 4,500 rpm for 5 min and the supernatant was collected, then the absorbance was measured at 280 nm. The lignin content was expressed as Absorption 280 on a fresh weight basis. All measurements were performed with three biological samples, and each sample was assayed in triplicate.

### Differentially Gene Expression (DGE) Library Construction and Sequencing

Young stigmas of about 1 mm in length were collected from WT and *ys* mutant at the same time on the same day. Samples were immediately frozen in liquid nitrogen and stored at –80°C for RNA-Seq analyses. Total RNA was isolated using the RNA extraction kit (Promega, United States). RNA quality was checked by RNase-free agarose gel electrophoresis to avoid possible degradation and contamination, and then verified using Agilent 2100 Bio-analyzer (Agilent Technologies, Santa Clara, CA, United States). Next, Poly (A) mRNA was isolated using oligo-dT beads (Qiagen, Germany), and then broken into short fragments by adding fragmentation buffer.

First-strand cDNA was synthesized using random hexamer-primed reverse transcription, followed by the synthesis of the second-strand cDNA using RNase H and DNA polymerase I. The cDNA fragments were purified using a QIA quick PCR extraction kit, and then washed with EB buffer for end repairation poly (A) addition and ligated to sequencing adapters. Following agarose gel electrophoresis and extraction of cDNA from gels, the cDNA fragments were purified and enriched by PCR to construct the final cDNA library, which was then sequenced on the Illumina sequencing platform (Illumina HiSeq™ 2500) using the paired-end technology. Three biological replicates were performed for each line from WT and *ys* mutant, thus six DGE libraries were generated and sequenced.

### Bioinformatics Analysis of DGE Data

Raw reads were filtered to remove low quality sequences (there were more than 50% bases with quality lower than 20 in one sequence), reads with more than 5% N bases (bases unknown) and reads containing adaptor sequences through the Perl program. Then the clean reads were mapped to the tomato reference genome using TopHat2 (Consortium, 2012; Kim D. et al., 2013), allowing up to one mismatch. Unigenes mapped by at least one read, in at least one sample, were identified for further analysis. The DEGs were identified using the R package edgeR (Robinson et al., 2010). The expression level of each unigene was calculated and normalized to FPKM. The FDR was used to determine the threshold of the P-value in multiple tests. In our study, the FDR < 0.05 and fold change > 2 were used as significance cut-offs of the gene expression differences.

Sequencing data were deposited to the Short Read Archive (SRA) database at the National Center for Biotechnology Information (NCBI) under the accession number SRP080654.

Further, the DEGs were used for GO and KEGG enrichment analyses according to Zhang et al. (2013). GO terms with corrected P-value < 0.05 and KEGG pathways with P-value < 0.05 were considered significantly enriched by differential expressed genes.

### Quantitative Real-Time PCR (qRT-PCR) Verification

Quantitative real-time PCR assays were performed using the independent tomato stigmas in the same developmental stage as those used for DGE analysis. Total RNA was isolated using the RNA extraction kit (Promega, United States), and cDNA was synthesized using MultiScribe reverse transcriptase (Applied Biosystems, United States). qRT-PCR was carried out using SYBR® *Premix Ex Taq*™ from TaKaRa (China) on an Applied Biosystems 7500 real-time PCR system (Applied Biosystems, United States). The tomato *EF-1 $\alpha$*  gene was used as reference gene to normalize the expression data. Each qRT-PCR experiment was repeated with three biological samples, and each sample was assayed in triplicate. The relative expression of genes was calculated using the  $2^{-\Delta\Delta\text{Ct}}$  method and standard error was calculated between three biological replicates. The

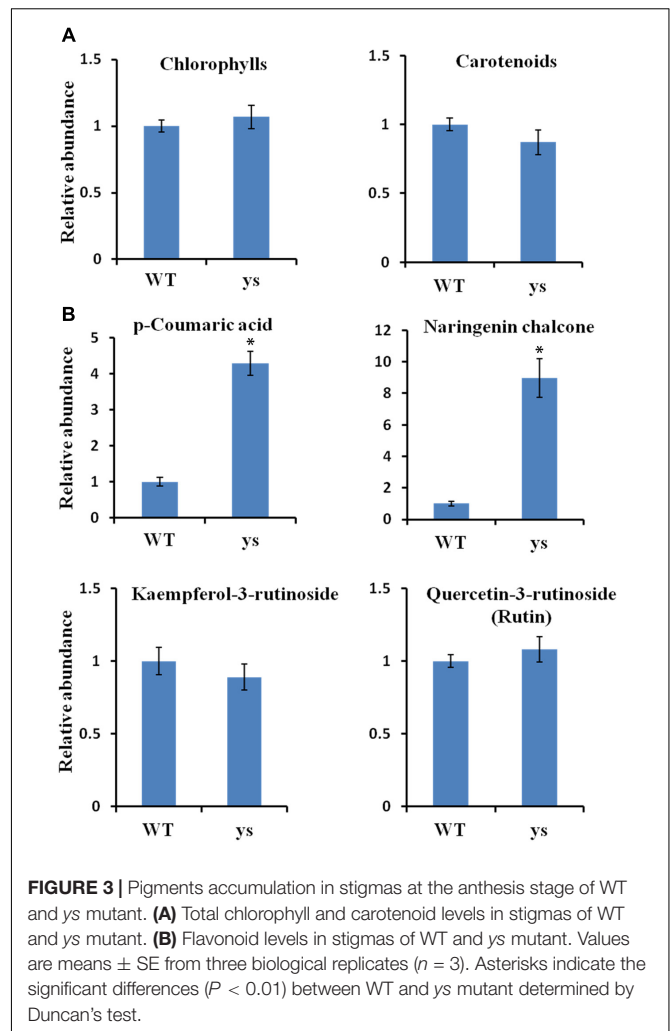
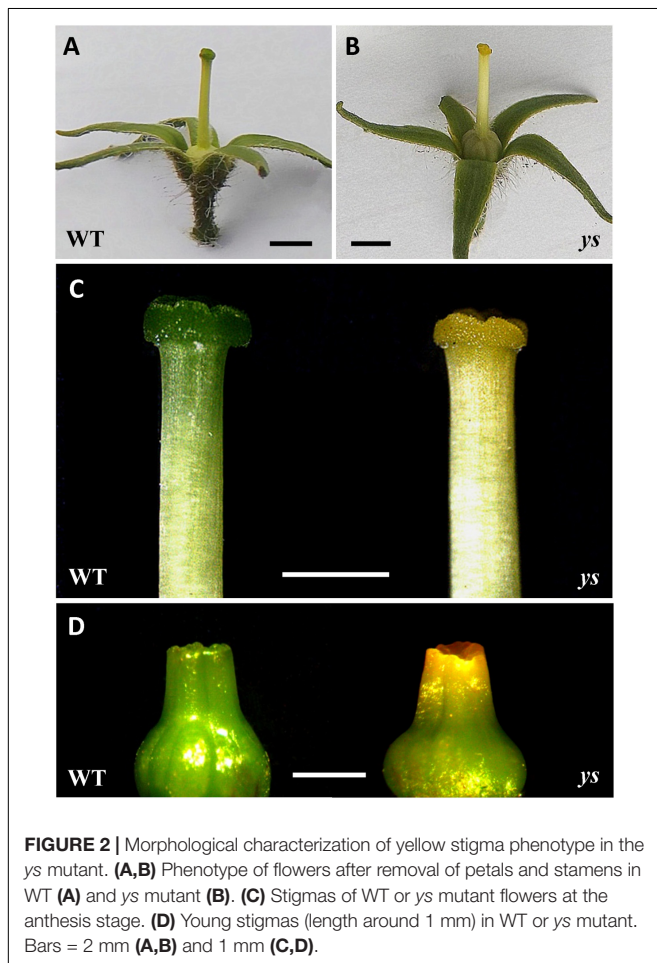
gene specific primers for qRT-PCR are listed in Supplementary Table S2.

## RESULTS

### Specific Flavonoid Accumulation Is Responsible for Yellow Stigma Phenotype in the *ys* Mutant

While the WT tomato plant was characterized by typical green stigma, the *ys* mutant, generated through EMS mutagenesis, showed unusual “yellow stigma” phenotype (Figures 2A–C). Notably, this stigma color difference between WT and *ys* mutant was apparent even in the very early stage of stigma development (stigma length around 1 mm) (Figure 2D).

To explore important pigments responsible for the “yellow stigma” phenotype, we quantified the contents of chlorophylls, carotenoids and flavonoids in the stigmas of WT and *ys* mutant during anthesis stage. To our surprise, no significant changes were noticed in both total chlorophyll and carotenoid levels between WT and *ys* mutant (Figure 3A and Supplementary Table S3). However, remarkable differences were found for some polyphenol contents in the flavonoid biosynthetic



pathway. For instance, the yellow stigma accumulated 4.3- and 8.9-fold increased *p*-coumaric acid and naringenin chalcone, respectively. However, the levels of kaempferol-3-rutinoside and quercetin-3-rutinoside (rutin) in stigmas were not changed between WT and *ys* mutant (Figure 3B and Supplementary Table S3). It is worth mentioning that the *p*-coumaric acid is a biosynthetic precursor of naringenin chalcone (Figure 1) (Petrucci et al., 2013; Saito et al., 2013; Falcone Ferreyra et al., 2015). Therefore, it is highly plausible that the higher accumulation of *p*-coumaric acid in the *ys* mutant led to an increased naringenin chalcone level. These results suggested that increased accumulation of yellow-colored flavonoid naringenin chalcone may be responsible for the yellow stigma phenotype in the *ys* mutant.

### Identification of Differentially Expressed Genes (DEGs) of Stigmas from WT and *ys* Mutant

To identify genes and gene networks that are involved in the formation of yellow stigma in tomato, we performed genome-wide expression analyses to compare the transcriptome

profiles of the stigmas between WT and *ys* mutant through the DGE approach (Eveland et al., 2010). Given that the phenotypic changes occurred in the early stage (Figure 2D), we chose young stigmas (length around 1 mm) for RNA-Seq analyses. In this project, 42.3–50.8 million raw reads from each DGE library were generated. After removal of adapter sequences and low-quality reads, we obtained 41.8–50.1 million high-quality clean reads with a total of 5.2–6.3 billion nucleotides. Among these clean reads, the percentage of Q20 (base quality more than 20) and GC was 94.4–94.8% and 42.8–43.0%, respectively (Supplementary Figure S1 and Table S4). Further, we clustered the clean reads into unique reads, which were mapped to the tomato genome using TopHat2 (Consortium, 2012; Kim D. et al., 2013). In the six DGE libraries, about 91.2–92.9% of clean reads from RNA-Seq data were mapped uniquely to the tomato genome (Supplementary Table S4).

Based on deep sequencing, 23,978 genes were detected in all libraries (Supplementary Table S5). We used the R package edgeR to identify the DEGs (Robinson et al., 2010). The expression level of each gene was normalized to FPKM. Using FDR < 0.05 and fold change > 2 as the significance cut-offs, we obtained 507 DEGs, in which 84 genes were significantly up-regulated and 423 genes were dramatically down-regulated in the stigmas of *ys* mutant as compared to those of WT plants (Supplementary Table S6). To validate the RNA-Seq data, we performed qRT-PCR assays using the independent tomato stigmas in the same developmental stage as those used for DGE analysis. Sixteen DEGs, including 6 up-regulated genes and 10 down-regulated genes, were randomly chosen for qRT-PCR analysis. As shown in Table 1, the qRT-PCR data were in full agreement with the RNA-Seq data in terms of relative fold change in the expression of these 16 genes between WT and *ys* mutant (Pearson correlation coefficient

0.969,  $P = 6.3E - 10$ ), suggesting that the RNA-Seq results were highly reliable.

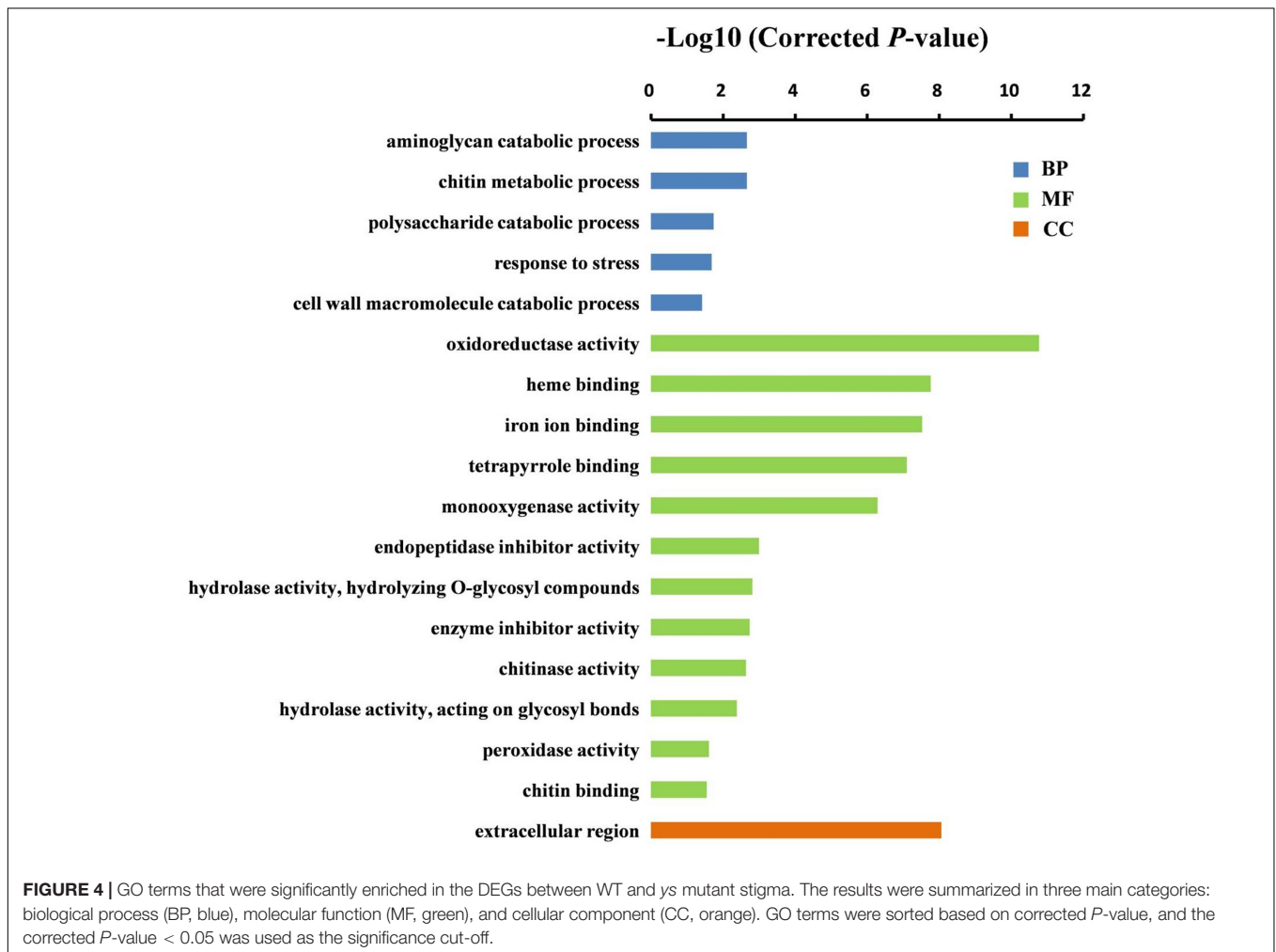
## Cytochrome P450s and Peroxidases Are Involved in the Formation of Yellow Stigma in Tomato

In order to understand the expression profiles and potential functions of DEGs identified by DGE, GO term enrichment analysis (corrected  $P$ -value < 0.05) was performed. The DEGs were classified into cellular component, biological process and molecular function categories (Supplementary Table S7). As shown in Figure 4, there was only one group “extracellular region” ( $P = 8.8E - 09$ ) in the cellular component category. The GO terms of catabolic and metabolic processes were dominantly enriched in the biological process group. In the molecular function category, the top three significantly enriched GO terms were “oxidoreductase activity” ( $P = 1.7E - 11$ ), “heme binding” ( $P = 1.7E - 08$ ) and “iron ion binding” ( $P = 3.0E - 08$ ). Interestingly, these three groups all shared 23 genes encoding cytochrome P450s (CYP450), a large family of enzymes that play a crucial role in the biosynthesis of flavonoids that are responsible for flower colors (Tanaka, 2006; Tanaka and Brugliera, 2013), and 10 genes encoding PODs (Supplementary Table S7), however, most of those genes were down-regulated in the stigmas of *ys* mutant compared to WT (Table 2). For example, the expression levels of two CYP450 genes, *Solyc10g078220* and *Solyc10g078230*, and two POD genes, *Solyc07g017880* and *Solyc02g084790*, decreased 139.8-, 130.8-, 54.9- and 28.2-fold, respectively, in the *ys* mutant compared with those in the WT, and qRT-PCR verification revealed the same expression pattern (Table 1). These data indicated that the cytochrome P450s and PODs may play important role in the formation of yellow stigma in tomato.

**TABLE 1** | qRT-PCR verification of differentially expressed genes identified by RNA-Seq.

Gene ID	Gene annotation	DGE FDR	DGE fold change ( <i>ys</i> vs. WT)	qRT-PCR fold change ( <i>ys</i> vs. WT)
Solyc12g008900	CKX6 (cytokinin oxidase 6)	1.02E - 04	21.32	14.84 ± 0.72
Solyc03g093890	MYB52 (R2R3-MYB domain protein 52)	3.65E - 02	14.50	11.08 ± 0.82
Solyc08g076820	bHLH146 (bHLH family protein 146)	4.60E - 02	13.29	18.56 ± 1.24
Solyc08g074620	PPO (polyphenol oxidase)	7.74E - 07	10.62	7.75 ± 0.67
Solyc10g055760	NAC6 (NAC domain protein 6)	6.36E - 06	10.27	6.88 ± 0.84
Solyc06g064840	AG (agamous MADS-box protein)	7.67E - 04	10.13	11.27 ± 1.50
Solyc10g078220	CYP450 (cytochrome P450)	5.23E - 07	-139.82	-62.69 ± 5.34
Solyc10g078230	CYP450 (cytochrome P450)	4.24E - 04	-130.78	-60.26 ± 6.35
Solyc07g056510	GST (glutathione S-transferase)	9.84E - 03	-86.87	-39.51 ± 4.43
Solyc07g017880	POD (peroxidase)	1.50E - 08	-54.91	-43.28 ± 3.39
Solyc02g084790	POD (peroxidase)	3.69E - 02	-28.24	-19.72 ± 4.25
Solyc01g109120	WD40 (WD40 repeat protein)	7.47E - 03	-8.83	-9.56 ± 1.58
Solyc07g056670	GA2OX2 (gibberellin 2-oxidase 2)	6.86E - 07	-8.14	-3.97 ± 0.56
Solyc06g083170	bHLH049 (bHLH family protein 049)	2.80E - 05	-4.96	-4.69 ± 0.58
Solyc01g100460	bZIP (bZIP domain protein)	5.00E - 03	-3.38	-5.26 ± 0.79
Solyc04g077010	RLK (receptor like kinase)	1.89E - 02	-2.98	-2.36 ± 0.27

The relative transcript level of each gene was expressed as the fold change between WT and *ys* mutant in the RNA-Seq data and qRT-PCR analyses. The tomato *EF-1a* gene was used as reference gene. The values shown represent the means ± SE from three biological replicates ( $n = 3$ ).

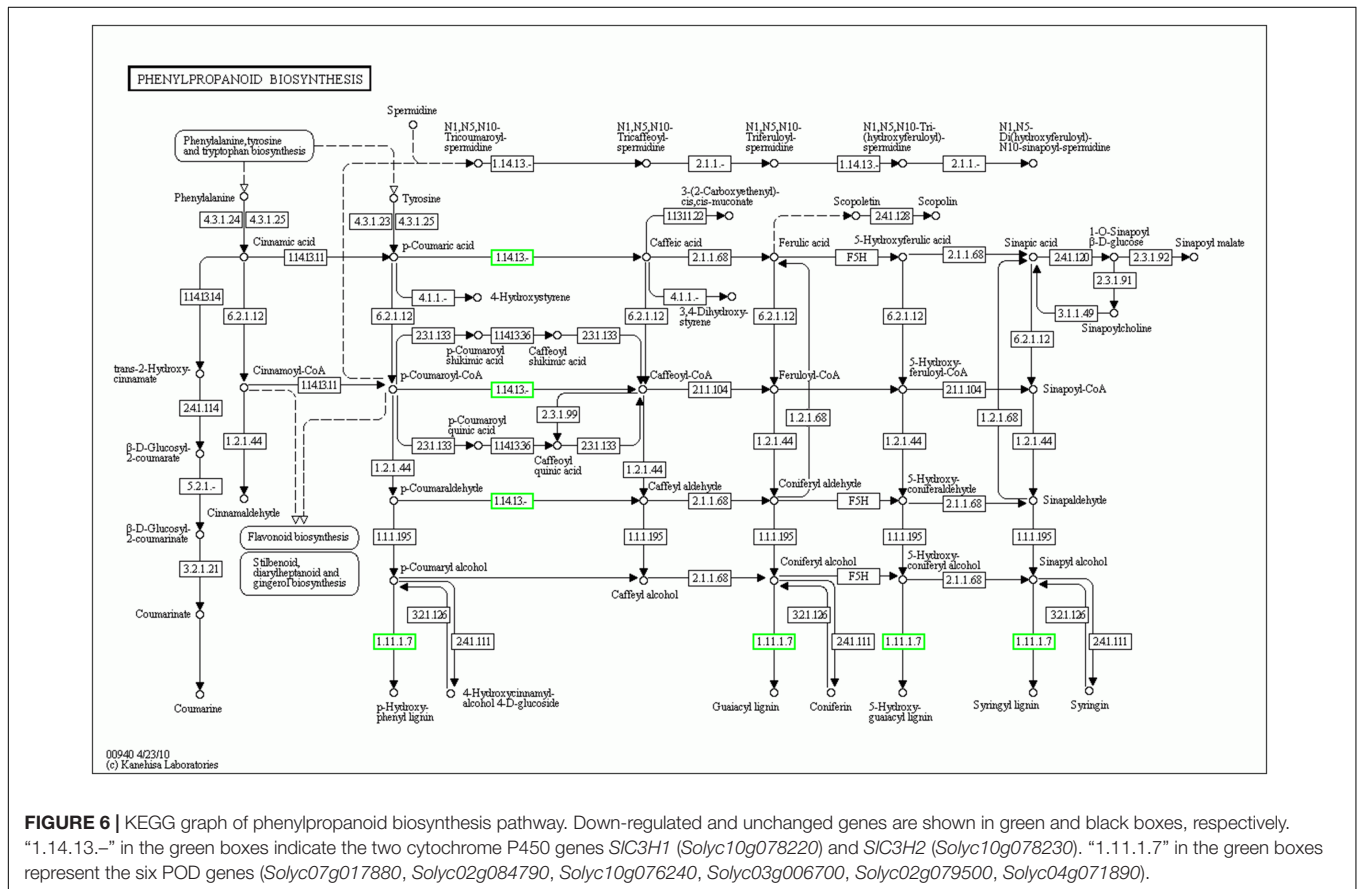
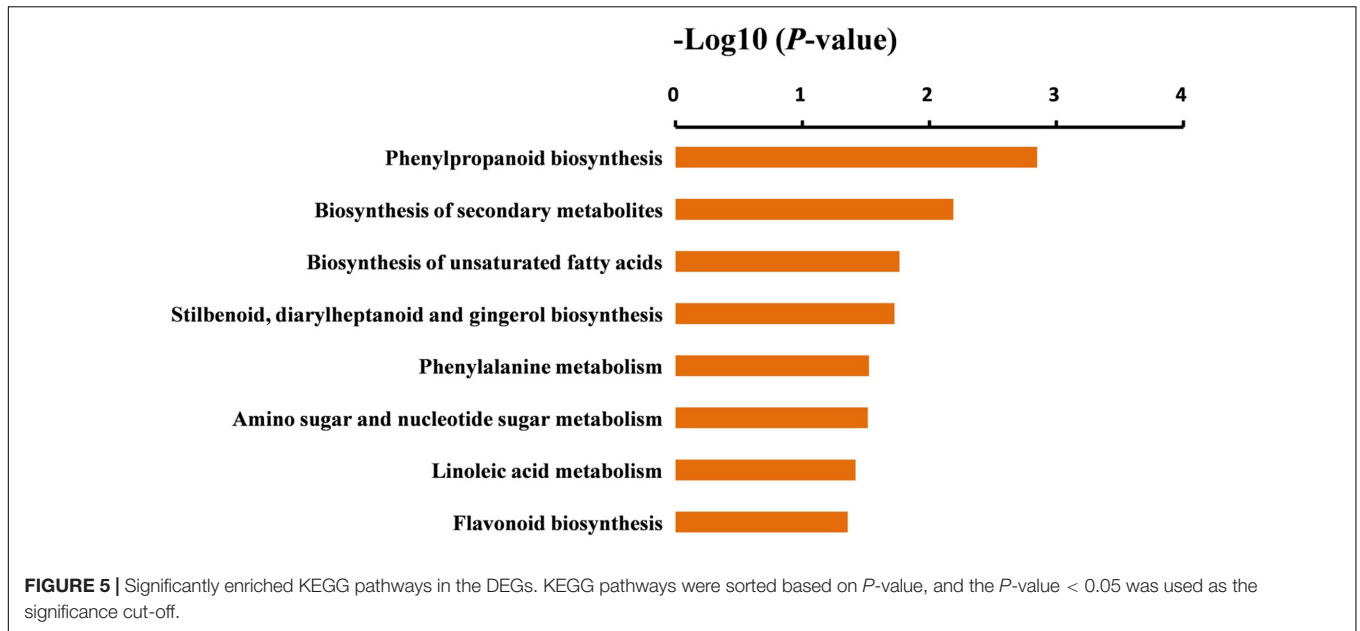


## Two Cytochrome P450 Genes and Six Peroxidase Genes May Function As Negative Regulators in Yellow Stigma Formation in Tomato

To further identify the biological pathways that are responsible for the formation of yellow stigma in tomato, we mapped the detected DEGs to reference canonical pathways in the KEGG (Kanehisa et al., 2004), and then compared these with the whole transcriptome background to search for genes involved in the metabolic or signal transduction pathways that were significantly enriched. Using the *P*-value < 0.05 as the significance cut-off, 29 DEGs, including 3 up-regulated and 26 down-regulated genes, were assigned to 8 KEGG pathways (Supplementary Table S8). Among them, the “Phenylpropanoid biosynthesis” ( $P = 1.4E - 03$ ), “Biosynthesis of secondary metabolites” ( $P = 6.5E - 03$ ) and “Biosynthesis of unsaturated fatty acids” ( $P = 1.7E - 02$ ) were the top three significantly enriched KEGG pathways (Figure 5). However, the “Flavonoid biosynthesis” pathway ( $P = 4.4E - 02$ ), which was putatively associated with the yellow stigma phenotype in the *ys* mutant (Figure 3B), was also enriched,

despite the *P*-value showed higher. Notably, two *CYP450* genes (*Solyc10g078220* and *Solyc10g078230*) and six *POD* genes (*Solyc07g017880*, *Solyc02g084790*, *Solyc10g076240*, *Solyc03g006700*, *Solyc02g079500*, and *Solyc04g071890*), whose expressions were dramatically down-regulated in the stigma of *ys* mutant (Table 2), were mapped into the “Phenylpropanoid biosynthesis” and “Biosynthesis of secondary metabolites” (Supplementary Table S8). Moreover, the two *CYP450* genes were also involved in the “Flavonoid biosynthesis” pathway (Supplementary Table S8). In these pathways, the two *CYP450* genes encoded the C3H which catalyze the *p*-coumaric acid, *p*-coumaroyl-CoA and *p*-coumaraldehyde to caffeic acid, caffeoyl-CoA and caffeoyl aldehyde, respectively (Figure 6 and Supplementary Figure S2) (Xue et al., 2014; Fornaléa et al., 2015), so, we named these two genes as *SIC3H1* (*Solyc10g078220*) and *SIC3H2* (*Solyc10g078230*). In addition, the six *POD* genes were involved in the last step of biosynthesis of lignin, an insoluble cell wall-associated polymer (Figure 6) (Quiroga et al., 2000; Higuchi, 2006).

It is worth mentioning that the *p*-coumaric acid acts as the common precursor for both flavonoid and lignin biosyntheses, and C3H and POD are two key enzymes in lignin biosynthetic



pathway (Higuchi, 2006; van der Rest et al., 2006; Petrusa et al., 2013; Renault et al., 2017). Given the repression of two *SIC3Hs* and six *PODs* in yellow stigma of the *ys* mutant (Table 2), we speculated that the higher accumulation of *p*-coumaric acid in

the *ys* mutant (Figure 3B) may result from the reduced lignin biosynthesis. To test this hypothesis, we compared the levels of caffeic acid, the downstream production of *p*-coumaric acid catalyzed by C3H and also a biosynthetic precursor of lignin

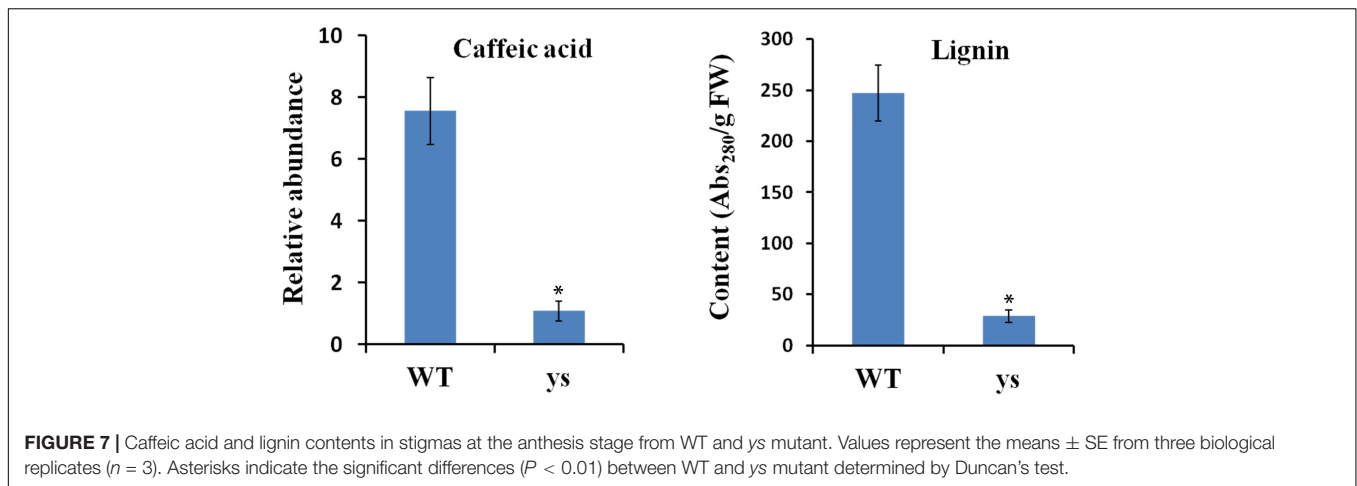


(Figure 6) (Higuchi, 2006; Renault et al., 2017), and lignin in the stigmas at anthesis stage between WT and *ys* mutant. As expected, the caffeic acid and lignin contents were 7.6- and 8.5-fold decreased in the *ys* mutant compared to those of WT, respectively (Figure 7 and Supplementary Table S3), suggesting that the reduced expressions of two *SIC3Hs* and six *PODs* might inhibit the biosynthesis of lignin, leading to a change in the direction of the metabolic flow of *p*-coumaric acid from lignin to flavonoid biosynthetic pathway, which eventually resulted in a higher naringenin chalcone level (Figure 3B). These observations indicated that the two *SIC3Hs* and six *PODs* may function as negative regulators in naringenin chalcone biosynthesis, which could play a positive role in yellow stigma formation in the *ys* mutant.

## DISCUSSION

The worldwide popularity of tomato as a fruit vegetable is due to its unique taste and high nutritional value, which are principally contributed by various pigments and secondary metabolites, such as flavonoids. Tomato fruits that display diverse colors upon maturation, are developed from floral organ, however, the colors of the different parts of flower remain essentially unchanged. For example, sepal, ovary, style, and stigma are green, while petal and anther are yellow all the time. Flower color plays a crucial role in attracting specific pollinators to facilitate pollination, which is essential for fertilization and subsequent fruit development. Therefore, it is important to better understand the mechanisms of pigmentation in different floral parts. However, previous studies with respect to regulatory mechanism of pigmentation in tomato have mainly been focused on fruits, and rarely on flowers or stigmas. In this study, we identified a *ys* mutant with unusual “yellow stigma” phenotype through EMS mutagenesis (Figure 2) (Saito et al., 2011). This study provides a useful basis for understanding the mechanism of pigment regulation in tomato stigma.

Chlorophylls, carotenoids, and flavonoids are the main three kinds of pigments in tomato (Ono et al., 2006; Tanaka and Brugliera, 2013). The color of ripe tomato fruit is mainly

determined by carotenoids and flavonoids, with the exception of specific genotypes (Ballester et al., 2010). While in this study, we found that chlorophylls and flavonoids are predominantly accumulated in the stigmas of both WT and *ys* mutant (Supplementary Table S3), suggesting that they play an important role in the formation of tomato stigma color. These observations also indicate an existence of similar as well as divergent pigment metabolism pathways between tomato stigma and fruit, while the flavonoids are involved in both processes. Furthermore, during the ripening process of tomato fruit, naringenin chalcone, one of the most abundant flavonoids in the fruit peel, is responsible for the yellow color at the breaker stage (Moco et al., 2006; Iijima et al., 2008; Ballester et al., 2010). In addition, the altered carotenoid compositions can also result in yellow color of fruit (Ballester et al., 2010). And in the stigma, naringenin chalcone functions as an activator for yellow stigma formation, owing to its significantly increased content detected in the *ys* mutant, but carotenoids do not affect stigma color because their accumulation is too much tiny and has no change between WT and *ys* (Figure 3 and Supplementary Table S3), supporting that carotenoids play different roles in yellow color formations of tomato stigma and fruit, while flavonoid naringenin chalcone is key in these two processes.

Lignin, a major component of secondary cell wall, can provide mechanical strength and also defend the vascular plants against biotic and abiotic stresses (Senthil-Kumar et al., 2010; Bi et al., 2011; Liu et al., 2016; Wang et al., 2017). Lignin is formed via the phenylpropanoid pathway and share common biosynthetic precursors with flavonoids, such as phenylalanine, cinnamic acid, and *p*-coumaric acid (Higuchi, 2006; van der Rest et al., 2006; Petrusa et al., 2013; Renault et al., 2017). Reduced lignin biosynthesis can enhance the availability of these precursors and, thereby, stimulate the production of flavonoid compounds. For example, up-regulation of cinnamate 4-hydroxylase (C4H), an enzyme catalyzed the synthesis of *p*-coumaric acid from cinnamic acid, shows opposite effects on the levels of stem lignin and fruit flavonoid, especially naringenin and rutin (Millar et al., 2007). Down-regulation of cinnamoyl-CoA reductase (CCR), a key enzyme in the formation of lignin monomers, results in decreased

**TABLE 2** | List of differentially expressed cytochrome P450 and POD genes identified by DGE in the stigmas of *ys* mutant and WT.

Gene ID	Fold Change ( <i>ys</i> /WT)	FDR
<b>Cytochrome P450s</b>		
Solyc03g122350	16.42	3.41E – 09
Solyc03g114940	14.32	7.69E – 06
Solyc12g006860	8.57	5.25E – 03
Solyc10g078220	–139.82	5.23E – 07
Solyc10g078230	–130.78	4.24E – 04
Solyc04g083140	–128.18	9.91E – 10
Solyc07g055560	–65.55	6.09E – 19
Solyc12g045020	–48.07	1.78E – 02
Solyc06g066230	–46.11	4.22E – 04
Solyc08g075320	–45.88	4.24E – 08
Solyc08g079420	–27.85	1.44E – 05
Solyc07g052370	–23.20	3.81E – 03
Solyc06g076160	–20.46	1.39E – 03
Solyc04g079660	–19.01	4.01E – 04
Solyc07g062500	–14.75	5.62E – 03
Solyc04g050620	–13.33	6.07E – 09
Solyc10g083690	–12.94	2.94E – 07
Solyc03g112030	–10.56	4.58E – 03
Solyc04g079640	–4.93	1.37E – 04
Solyc07g055460	–4.52	9.34E – 03
Solyc04g078900	–2.78	1.89E – 02
Solyc09g098610	–2.75	1.27E – 02
Solyc10g087040	–2.25	2.34E – 02
<b>Peroxidases</b>		
Solyc01g006300	–9990.00	4.49E – 03
Solyc02g087070	–102.67	3.03E – 03
Solyc07g017880	–54.91	1.50E – 08
Solyc02g094180	–53.14	5.27E – 06
Solyc01g105070	–43.48	1.76E – 06
Solyc02g084790	–28.24	3.69E – 02
Solyc10g076240	–21.33	2.98E – 07
Solyc03g006700	–9.45	5.00E – 03
Solyc02g079500	–3.04	1.77E – 02
Solyc04g071890	–2.17	4.26E – 02

lignin content and higher amounts of chlorogenic acid, rutin and kaempferol rutinoside in tomato (van der Rest et al., 2006). And in this article, through RNA-Seq and biochemical analyses, we demonstrated that repression of C3H and POD, which are thought to be essential for lignin biosynthesis (Quiroga et al., 2000; Franke et al., 2002; Higuchi, 2006), leads to reduced lignin accumulation and increased *p*-coumaric acid and naringenin chalcone levels (Figures 3, 7 and Table 2), which has similar interaction model between lignin and flavonoid as previous studies, but different effects on flavonoid compounds.

In fact, the roles of C3H gene in flavonoid metabolism and plant color have been verified previously. For instance, C3Hs participate in the biosynthesis of chlorogenic acid (Mahesh et al., 2007; Kim Y.B. et al., 2013). And repression of C3Hs in *Arabidopsis* and maize increases the accumulation of anthocyanins, leading to purple coloration in their leaves (Abdulrazzak et al., 2006; Fornaléa et al., 2015). Moreover,

extensive studies have been performed in the regulation of POD genes on plant responses to stress, but the involvement of PODs in plant color control has never been reported. Therefore, our results strengthen the theory of regulation of C3Hs in flavonoid pathway and provide a new perspective of the effect of C3Hs and PODs on naringenin chalcone, contributing to the yellowing of stigma color in tomato. As it stands now, our understanding of the biological functions of two *SIC3H1s* and six *PODs* is based on bioinformatic and biochemical analyses, therefore, further study is to be carried out to elucidate their specific roles in tomato stigma color formation by expression pattern analysis and genetic transformation study (RNAi and overexpression) in tomato. As such, our data provide valuable information for further functional characterization of yellow stigma phenotype.

Furthermore, the transcriptional regulation of flavonoid and lignin biosyntheses is controlled by some key TFs in plants. For instance, R2R3-MYB, bHLH, and WDR participate in flavonoid biosynthetic pathway (Xu et al., 2014, 2015), while KNOX, HD-ZIP, NAC, and R2R3-MYB are involved in the regulation of lignin (Du et al., 2011; Xu et al., 2012; Townsley et al., 2013; Liu et al., 2015). It appears that R2R3-MYB factors potentially play key roles in both pathways. Further, some members of this family have been recognized as positive regulators of flavonoid biosynthesis. For example, AtMYB11, AtMYB12, and AtMYB111 in *Arabidopsis* can activate flavonoid biosynthetic genes, and overexpression of *AtMYB11* or *AtMYB12* enhances the flavonol content (Mehrtens et al., 2005; Li et al., 2015; Liu et al., 2015). In tomato, deregulated expression of *SIMYB12* results in a decreased level of naringenin chalcone, leading to pink fruit color (Ballester et al., 2010). Moreover, several R2R3-MYB TFs have been identified as repressors of lignin biosynthetic pathway. For instance, ZmMYB31 and ZmMYB42 of maize suppress several lignin genes, thereby reducing the lignin content, and this effect redirects the phenylpropanoid metabolic flux toward the biosynthesis of flavonoid (Sonbol et al., 2009; Fornale et al., 2010). And MYBs from other species such as snapdragon (*Antirrhinum majus*), switchgrass (*Panicum virgatum*) and leucaena (*Leucaena leucocephala*) can also inhibit lignin biosynthesis (Liu et al., 2015). In our study, given the blocked lignin biosynthetic pathway and increased accumulation of flavonoids in the stigma of *ys* mutant (Figures 3B, 7), we speculate that the shift in the expression profile of C3Hs and PODs may also be regulated by R2R3-MYB TFs, however, this hypothesis needs to be confirmed in the future.

In addition, given the importance of stigma in pollination of flowering plants, we tried to explore the effect of this stigma color mutation on reproductive development in tomato, but disappointingly, we did not find any significant difference between WT and *ys* mutant in terms of stigma receptivity, pollen viability, pollination, and fruit set (data not shown). Even so, the discovery and description of *ys* phenotype have important scientific and theoretical significances in understanding the mechanism of tomato stigma color development, which has never been reported before our study, and improving the pigment regulation in tomato plants. Given that both flavonoids and lignin play important roles in plant responses to environmental stress (Senthil-Kumar et al., 2010; Petrusa et al., 2013; Zhang et al., 2015; Liu et al., 2016), and their contents are changed in

the *ys* mutant as compared to those of WT (Figures 3, 7), in future work, we will explore the importance of stigma color in term of interaction between pigments and environmental factors in tomato.

## AUTHOR CONTRIBUTIONS

YZ and YaL designed the experiments, YZ, GZ, JZ, and MS performed the experiments. YZ, GZ, YuL, and TM analyzed the data. YZ wrote the paper along with YaL. All authors reviewed the manuscript.

## FUNDING

This work was supported by the National Key Research and Development Program of China (2016YFD0101703) to YaL and

## REFERENCES

- Abdulrazzak, N., Pollet, B., Ehling, J., Larsen, K., Asnaghi, C., Ronseau, S., et al. (2006). A coumaroyl-ester-3-hydroxylase insertion mutant reveals the existence of nonredundant meta-hydroxylation pathways and essential roles for phenolic precursors in cell expansion and plant growth. *Plant Physiol.* 140, 30–48. doi: 10.1104/pp.105.069690
- Ballester, A. R., Molthoff, J., de Vos, R., Hekkert, B., Orzaez, D., Fernandez-Moreno, J. P., et al. (2010). Biochemical and molecular analysis of pink tomatoes: deregulated expression of the gene encoding transcription factor SIMYB12 leads to pink tomato fruit color. *Plant Physiol.* 152, 71–84. doi: 10.1104/pp.109.147322
- Baudry, A., Heim, M. A., Dubreucq, B., Caboche, M., Weisshaar, B., and Lepiniec, L. (2004). TT2, TT8, and TTG1 synergistically specify the expression of *BANYULS* and proanthocyanidin biosynthesis in *Arabidopsis thaliana*. *Plant J.* 39, 366–380. doi: 10.1111/j.1365-313X.2004.02138.x
- Bi, C., Chen, F., Jackson, L., Gill, B. S., and Li, W. (2011). Expression of lignin biosynthetic genes in wheat during development and upon infection by fungal pathogens. *Plant Mol. Biol. Rep.* 29, 149–161. doi: 10.1007/s11105-010-0219-8
- Bino, R. J., de Vos, C. H. R., Lieberman, M., Hall, R. D., Bovy, A., Jonker, H. H., et al. (2005). The light-hyperresponsive *high pigment-2<sup>dh</sup>* mutation of tomato: alterations in the fruit metabolome. *New Phytol.* 166, 427–438. doi: 10.1111/j.1469-8137.2005.01362.x
- Bou-Torrent, J., Toledo-Ortiz, G., Ortiz-Alcaide, M., Cifuentes-Esquivel, N., Halliday, K. J., Martinez-Garcia, J. F., et al. (2015). Regulation of carotenoid biosynthesis by shade relies on specific subsets of antagonistic transcription factors and cofactors. *Plant Physiol.* 169, 1584–1594. doi: 10.1104/pp.15.00552
- Bovy, A., de Vos, R., Kemper, M., Schijlen, E., Almenar Pertejo, M., Muir, S., et al. (2002). High-flavonol tomatoes resulting from the heterologous expression of the maize transcription factor genes *LC* and *C1*. *Plant Cell* 14, 2509–2526. doi: 10.1105/tpc.004218
- Buer, C. S., and Djordjevic, M. A. (2009). Architectural phenotypes in the *transparent testa* mutants of *Arabidopsis thaliana*. *J. Exp. Bot.* 60, 751–763. doi: 10.1093/jxb/ern323
- Buer, C. S., Imin, N., and Djordjevic, M. A. (2010). Flavonoids: new roles for old molecules. *J. Integr. Plant Biol.* 52, 98–111. doi: 10.1111/j.1744-7909.2010.00905.x
- Buer, C. S., Muday, G. K., and Djordjevic, M. A. (2007). Flavonoids are differentially taken up and transported long distances in *Arabidopsis*. *Plant Physiol.* 145, 478–490. doi: 10.1104/pp.107.101824
- Colliver, S., Bovy, A., Collins, G., Muir, S., Robinson, S., de Vos, C. H. R., et al. (2002). Improving the nutritional content of tomatoes through reprogramming their flavonoid biosynthetic pathway. *Phytochem. Rev.* 1, 113–123.

by the National Key Research and Development Program of China (2016YFD0100204-30), Science and Technology Research and Development Program of Shaanxi Province (2015NY098) and Fundamental Research Funds for Northwest A&F University (2452015024) to YZ.

## ACKNOWLEDGMENT

We thank members of the Liang laboratory for helpful discussions and technical assistance.

## SUPPLEMENTARY MATERIAL

The Supplementary Material for this article can be found online at: <http://journal.frontiersin.org/article/10.3389/fpls.2017.00897/full#supplementary-material>

- Consortium, T. G. (2012). The tomato genome sequence provides insights into fleshy fruit evolution. *Nature* 485, 635–641. doi: 10.1038/nature11119
- Du, J., Miura, E., Robischon, M., Martinez, C., and Groover, A. (2011). The *Populus* Class III HD ZIP transcription factor *POPCORONA* affects cell differentiation during secondary growth of woody stems. *PLoS ONE* 6:e17458. doi: 10.1371/journal.pone.0017458
- Dubos, C., Stracke, R., Grotewold, E., Weisshaar, B., Martin, C., and Lepiniec, L. (2010). MYB transcription factors in *Arabidopsis*. *Trends Plant Sci.* 15, 573–581. doi: 10.1016/j.tplants.2010.06.005
- Eveland, A. L., Satoh-Nagasawa, N., Goldshmidt, A., Meyer, S., Beatty, M., Sakai, H., et al. (2010). Digital gene expression signatures for maize development. *Plant Physiol.* 154, 1024–1039. doi: 10.1104/pp.110.159673
- Falcone Ferreyra, M. L., Emiliani, J., Rodriguez, E. J., Campos-Bermudez, V. A., Grotewold, E., and Casati, P. (2015). The identification of maize and *Arabidopsis* type I FLAVONE SYNTHASEs links flavones with hormones and biotic interactions. *Plant Physiol.* 169, 1090–1107. doi: 10.1104/pp.15.00515
- Feller, A., Machemer, K., Braun, E. L., and Grotewold, E. (2011). Evolutionary and comparative analysis of MYB and bHLH plant transcription factors. *Plant J.* 66, 94–116. doi: 10.1111/j.1365-313X.2010.04459.x
- Fornale, S., Shi, X., Chai, C., Encina, A., Irar, S., Capellades, M., et al. (2010). ZmMYB31 directly represses maize lignin genes and redirects the phenylpropanoid metabolic flux. *Plant J.* 64, 633–644. doi: 10.1111/j.1365-313X.2010.04363.x
- Fornaléa, S., Rencoret, J., Garcia-Calvo, L., Capellades, M., Encina, A., Santiago, R., et al. (2015). Cell wall modifications triggered by the down-regulation of Coumarate 3-hydroxylase-1 in maize. *Plant Sci.* 236, 272–282. doi: 10.1016/j.plantsci.2015.04.007
- Franke, R., Humphreys, J. M., Hemm, M. R., Denault, J. W., Ruegger, M. O., Cusumano, J. C., et al. (2002). The *Arabidopsis* *REF8* gene encodes the 3-hydroxylase of phenylpropanoid metabolism. *Plant J.* 30, 33–45. doi: 10.1046/j.1365-313X.2002.01266.x
- Gao, L., Yang, H., Liu, H., Yang, J., and Hu, Y. (2016). Extensive transcriptome changes underlying the flower color intensity variation in *Paeonia ostii*. *Front. Plant Sci.* 6:1205. doi: 10.3389/fpls.2015.01205
- Gonzalez, A., Zhao, M., Leavitt, J. M., and Lloyd, A. M. (2008). Regulation of the anthocyanin biosynthetic pathway by the TTG1/bHLH/Myb transcriptional complex in *Arabidopsis* seedlings. *Plant J.* 53, 814–827. doi: 10.1111/j.1365-313X.2007.03373.x
- Gonzali, S., Mazzucato, A., and Perata, P. (2009). Purple as a tomato: towards high anthocyanin tomatoes. *Trends Plant Sci.* 14, 237–241. doi: 10.1016/j.tplants.2009.02.001
- Grotewold, E. (2006). The genetics and biochemistry of floral pigments. *Annu. Rev. Plant Biol.* 57, 761–780. doi: 10.1146/annurev.arplant.57.032905.105248

- Han, L., Zhang, T., Xu, J., Li, Y., Wang, X., and Wu, X. (2006). Genetic analysis and gene mapping of purple stigma in rice. *Acta Genet. Sin.* 33, 642–646.
- Hannun, S. M. (2004). Potential impact of strawberries on human health: a review of the science. *Crit. Rev. Food Sci. Nutr.* 44, 1–17. doi: 10.1080/10408690490263756
- Harborne, J. B., and Williams, C. A. (2000). Advances in flavonoid research since 1992. *Phytochemistry* 55, 481–504.
- Heim, M. A., Jakoby, M., Werber, M., Martin, C., Weisshaar, B., and Bailey, P. C. (2003). The basic helix-loop-helix transcription factor family in plants: a genome-wide study of protein structure and functional diversity. *Mol. Biol. Evol.* 20, 735–747. doi: 10.1093/molbev/msg088
- Higuchi, T. (2006). Look back over the studies of lignin biochemistry. *J. Wood Sci.* 52, 2–8. doi: 10.1007/s10086-005-0790-z
- Hooper, L., and Cassidy, A. (2006). A review of the health care potential of bioactive compounds. *J. Sci. Food Agric.* 86, 1805–1813. doi: 10.1002/jfsa.2599
- Iijima, Y., Nakamura, Y., Ogata, Y., Tanaka, K., Sakurai, N., Suda, K., et al. (2008). Metabolite annotations based on the integration of mass spectral information. *Plant J.* 54, 949–962. doi: 10.1111/j.1365-313X.2008.03434.x
- Julkunen-Tiitto, R., Nenadis, N., Neugart, S., Robson, M., Agati, G., Vepsäläinen, J., et al. (2015). Assessing the response of plant flavonoids to UV radiation: an overview of appropriate techniques. *Phytochem. Rev.* 14, 273–297. doi: 10.1007/s11101-014-9362-4
- Kanehisa, M., Goto, S., Kawashima, S., Okuno, Y., and Hattori, M. (2004). The KEGG resource for deciphering the genome. *Nucleic Acids Res.* 32, D277–D280.
- Kim, D., Pertea, G., Trapnell, C., Pimentel, H., Kelley, R., and Salzberg, S. L. (2013). TopHat2: accurate alignment of transcriptomes in the presence of insertions, deletions and gene fusions. *Genome Biol.* 14:R36. doi: 10.1186/gb-2013-14-4-r36
- Kim, Y. B., Thwe, A. A., Kim, Y. J., Li, X., Kim, H. H., Park, P. B., et al. (2013). Characterization of genes for a putative hydroxycinnamoyl-coenzyme A quinate transferase and *p*-coumarate 3'-hydroxylase and chlorogenic acid accumulation in tartary buckwheat. *J. Agric. Food Chem.* 61, 4120–4126. doi: 10.1021/jf4000659
- Koes, R., Verweij, W., and Quattrocchio, F. (2005). Flavonoids: a colorful model for the regulation and evolution of biochemical pathways. *Trends Plant Sci.* 10, 236–242. doi: 10.1016/j.tplants.2005.03.002
- Kuhn, B. M., Geisler, M., Bigler, L., and Ringli, C. (2011). Flavonols accumulate asymmetrically and affect auxin transport in *Arabidopsis*. *Plant Physiol.* 156, 585–595. doi: 10.1104/pp.111.175976
- Li, Q., Zhao, P., Li, J., Zhang, C., Wang, L., and Ren, Z. (2014). Genome-wide analysis of the WD-repeat protein family in cucumber and *Arabidopsis*. *Mol. Genet. Genomics* 289, 103–124. doi: 10.1007/s00438-013-0789-x
- Li, Y., Chen, M., Wang, S., Ning, J., Ding, X., and Chu, Z. (2015). *AtMYB11* regulates caffeoylquinic acid and flavonol synthesis in tomato and tobacco. *Plant Cell Tissue Organ Cult.* 122, 309–319. doi: 10.1007/s11240-015-0767-6
- Lichtenthaler, H. K. (1987). Chlorophylls and carotenoids: pigments of photosynthetic biomembranes. *Methods Enzymol.* 148, 350–382.
- Liu, H., Guo, Z., Gu, F., Ke, S., Sun, D., Dong, S., et al. (2016). 4-coumarate-CoA ligase-like gene *OsAAE3* negatively mediates the rice blast resistance, floret development and lignin biosynthesis. *Front. Plant Sci.* 7:2041. doi: 10.3389/fpls.2016.02041
- Liu, J., Osbourn, A., and Ma, P. (2015). MYB transcription factors as regulators of phenylpropanoid metabolism in plants. *Mol. Plant* 8, 689–708. doi: 10.1016/j.molp.2015.03.012
- Mahesh, V., Million-Rousseau, R., Ullmann, P., Chabrilange, N., Bustamante, J., Mondolot, L., et al. (2007). Functional characterization of two *p*-coumaroyl ester 3'-hydroxylase genes from coffee tree: evidence of a candidate for chlorogenic acid biosynthesis. *Plant Mol. Biol.* 64, 145–159. doi: 10.1007/s11103-007-9141-3
- Martin, C., Butelli, E., Petroni, K., and Tonelli, C. (2011). How can research on plants contribute to promoting human health. *Plant Cell* 23, 1685–1699. doi: 10.1105/tpc.111.083279
- Mehrtens, F., Kranz, H., Bednarek, P., and Weisshaar, B. (2005). The *Arabidopsis* transcription factor MYB12 is a flavonol-specific regulator of phenylpropanoid biosynthesis. *Plant Physiol.* 138, 1083–1096. doi: 10.1104/pp.104.058032
- Millar, D. J., Long, M., Donovan, G., Fraser, P. D., Boudet, A. M., Danoun, S., et al. (2007). Introduction of sense constructs of cinnamate 4-hydroxylase (CYP73A24) in transgenic tomato plants shows opposite effects on flux into stem lignin and fruit flavonoids. *Phytochemistry* 68, 1497–1509. doi: 10.1016/j.phytochem.2007.03.018
- Moco, S., Bino, R. J., Vorst, O., Verhoeven, H. A., de Groot, J., van Beek, T. A., et al. (2006). A liquid chromatography-mass spectrometry-based metabolome database for tomato. *Plant Physiol.* 141, 1205–1218. doi: 10.1104/pp.106.078428
- Morita, Y., Saitoh, M., Hoshino, A., Nitasaka, E., and Iida, S. (2006). Isolation of cDNAs for R2R3-MYB, bHLH and WDR transcriptional regulators and identification of *c* and *ca* mutations conferring white flowers in the Japanese morning glory. *Plant Cell Physiol.* 47, 457–470. doi: 10.1093/pcp/pcj012
- Ono, E., Fukuchi-Mizutani, M., Nakamura, N., Fukui, Y., Yonekura-Sakakibara, K., Yamaguchi, M., et al. (2006). Yellow flowers generated by expression of the aureone biosynthetic pathway. *Proc. Natl. Acad. Sci. U.S.A.* 103, 11075–11080. doi: 10.1073/pnas.0604246103
- Owens, D. K., Alerding, A. B., Crosby, K. C., Bandara, A. B., Westwood, J. H., and Winkel, B. S. (2008a). Functional analysis of a predicted flavonol synthase gene family in *Arabidopsis*. *Plant Physiol.* 147, 1046–1061. doi: 10.1104/pp.108.117457
- Owens, D. K., Crosby, K. C., Runac, J., Howard, B. A., and Winkel, B. S. (2008b). Biochemical and genetic characterization of *Arabidopsis* flavanone 3β-hydroxylase. *Plant Physiol. Biochem.* 46, 833–843. doi: 10.1016/j.plaphy.2008.06.004
- Petrussa, E., Braidot, E., Zancani, M., Peresson, C., Bertolini, A., Patui, S., et al. (2013). Plant flavonoids-biosynthesis, transport and involvement in stress responses. *Int. J. Mol. Sci.* 14, 14950–14973. doi: 10.3390/ijms140714950
- Pourcel, L., Routaboul, J. M., Kerhoas, L., Caboche, M., Lepiniec, L., and Debeaujon, I. (2005). *TRANSPARENT TESTA10* encodes a laccase-like enzyme involved in oxidative polymerization of flavonoids in *Arabidopsis* seed coat. *Plant Cell* 17, 2966–2980. doi: 10.1105/tpc.105.035154
- Quiroga, M., Guerrero, C., Botella, M. A., Barceló, A., Amaya, I., Medina, M. I., et al. (2000). A tomato peroxidase involved in the synthesis of lignin and suberin. *Plant Physiol.* 122, 1119–1127.
- Ramsay, N. A., and Glover, B. J. (2005). MYB-bHLH-WD40 protein complex and the evolution of cellular diversity. *Trends Plant Sci.* 10, 63–70. doi: 10.1016/j.tplants.2004.12.011
- Renault, H., Alber, A., Horst, N. A., Basilio Lopes, A., Fich, E. A., Kriegshausler, L., et al. (2017). A phenol-enriched cuticle is ancestral to lignin evolution in land plants. *Nat. Commun.* 8:14713. doi: 10.1038/ncomms14713
- Robinson, M. D., McCarthy, D. J., and Smyth, G. K. (2010). edgeR: a Bioconductor package for differential expression analysis of digital gene expression data. *Bioinformatics* 26, 139–140. doi: 10.1093/bioinformatics/btp616
- Saito, K., Yonekura-Sakakibara, K., Nakabayashi, R., Higashi, Y., Yamazaki, M., Tohge, T., et al. (2013). The flavonoid biosynthetic pathway in *Arabidopsis*: structural and genetic diversity. *Plant Physiol. Biochem.* 72, 21–34. doi: 10.1016/j.plaphy.2013.02.001
- Saito, T., Ariizumi, T., Okabe, Y., Asamizu, E., Hiwasa-Tanase, K., Fukuda, N., et al. (2011). TOMATOMA: a novel tomato mutant database distributing Micro-Tom mutant collections. *Plant Cell Physiol.* 52, 283–296. doi: 10.1093/pcp/pcr004
- Senthil-Kumar, M., Hema, R., Suryachandra, T. R., Ramegowda, H. V., Gopalakrishna, R., Rama, N., et al. (2010). Functional characterization of three water deficit stress-induced genes in tobacco and *Arabidopsis*: an approach based on gene down regulation. *Plant Physiol. Biochem.* 48, 35–44. doi: 10.1016/j.plaphy.2009.09.005
- Shirley, B. W., Kuhasek, W. L., Storz, G., Bruggemann, E., Koornneef, M., Ausubel, F. M., et al. (1995). Analysis of *Arabidopsis* mutants deficient in flavonoid biosynthesis. *Plant J.* 8, 659–671.
- Sonbol, F. M., Fornale, S., Capellades, M., Encina, A., Tourino, S., Torres, J. L., et al. (2009). The maize ZmMYB42 represses the phenylpropanoid pathway and affects the cell wall structure, composition and degradability in *Arabidopsis thaliana*. *Plant Mol. Biol.* 70, 283–296. doi: 10.1007/s11103-009-9473-2
- Tanaka, Y. (2006). Flower colour and cytochromes P450. *Phytochem. Rev.* 5, 283–291. doi: 10.1007/s11101-006-9003-7
- Tanaka, Y., and Brugliera, F. (2013). Flower colour and cytochromes P450. *Philos. Trans. R. Soc. Lond. B Biol. Sci.* 368:20120432. doi: 10.1098/rstb.2012.0432

- Tanaka, Y., Sasaki, N., and Ohmiya, A. (2008). Biosynthesis of plant pigments: anthocyanins, betalains and carotenoids. *Plant J.* 54, 733–749. doi: 10.1111/j.1365-3113.2008.03447.x
- Tapas, A. R., Sakarkar, D. M., and Kakde, R. B. (2008). Flavonoids as nutraceuticals: a review. *Trop. J. Pharm. Res.* 7, 1089–1099.
- Thevenin, J., Dubos, C., Xu, W., Le Gourrierc, J., Kelemen, Z., Charlot, F., et al. (2012). A new system for fast and quantitative analysis of heterologous gene expression in plants. *New Phytol.* 193, 504–512. doi: 10.1111/j.1469-8137.2011.03936.x
- Townsley, B. T., Sinha, N. R., and Kang, J. (2013). KNOX1 genes regulate lignin deposition and composition in monocots and dicots. *Front. Plant Sci.* 4:121. doi: 10.3389/fpls.2013.00121
- van der Rest, B., Danoun, S., Boudet, A. M., and Rochange, S. F. (2006). Down-regulation of cinnamoyl-CoA reductase in tomato (*Solanum lycopersicum* L.) induces dramatic changes in soluble phenolic pools. *J. Exp. Bot.* 57, 1399–1411. doi: 10.1093/jxb/erj120
- Wang, Z., Ge, Q., Chen, C., Jin, X., Cao, X., and Wang, Z. (2017). Function analysis of caffeoyl-CoA O-methyltransferase for biosynthesis of lignin and phenolic acid in *Salvia miltiorrhiza*. *Appl. Biochem. Biotechnol.* 181, 562–572. doi: 10.1007/s12010-016-2231-4
- Weston, L. A., and Mathesius, U. (2013). Flavonoids: their structure, biosynthesis and role in the rhizosphere, including allelopathy. *J. Chem. Ecol.* 39, 283–297. doi: 10.1007/s10886-013-0248-5
- Winkel, B. S. J. (2004). Metabolic channeling in plants. *Annu. Rev. Plant Biol.* 55, 85–107. doi: 10.1146/annurev.arplant.55.031903.141714
- Xu, B., Sathitsuksanoh, N., Tang, Y., Udvardi, M. K., Zhang, J. Y., Shen, Z., et al. (2012). Overexpression of *AtLOV1* in Switchgrass alters plant architecture, lignin content, and flowering time. *PLoS ONE* 7:e47399. doi: 10.1371/journal.pone.0047399
- Xu, W., Dubos, C., and Lepiniec, L. (2015). Transcriptional control of flavonoid biosynthesis by MYB-bHLH-WDR complexes. *Trends Plant Sci.* 20, 176–185. doi: 10.1016/j.tplants.2014.12.001
- Xu, W., Grain, D., Bobet, S., Le Gourrierc, J., Thevenin, J., Kelemen, Z., et al. (2014). Complexity and robustness of the flavonoid transcriptional regulatory network revealed by comprehensive analyses of MYB-bHLH-WDR complexes and their targets in *Arabidopsis* seed. *New Phytol.* 202, 132–144. doi: 10.1111/nph.12620
- Xue, Y., Zhang, Y., Grace, S., and He, Q. (2014). Functional expression of an *Arabidopsis* p450 enzyme, *p*-coumarate-3-hydroxylase, in the cyanobacterium *Synechocystis* PCC 6803 for the biosynthesis of caffeic acid. *J. Appl. Phycol.* 26, 219–226. doi: 10.1007/s10811-013-0113-5
- Yan, L., Liu, S., Zhao, S., Kang, Y., Wang, D., Gu, T., et al. (2012). Identification of differentially expressed genes in sorghum (*Sorghum bicolor*) brown midrib mutants. *Physiol. Plant.* 146, 375–387. doi: 10.1111/j.1399-3054.2012.01646.x
- Ye, J., Hu, T., Yang, C., Li, H., Yang, M., Ijaz, R., et al. (2015). Transcriptome profiling of tomato fruit development reveals transcription factors associated with ascorbic acid, carotenoid and flavonoid biosynthesis. *PLoS ONE* 10:e0130885. doi: 10.1371/journal.pone.0130885
- Zhang, J., Wu, K., Zeng, S., da Silva, J. A. T., Zhao, X., Tian, C., et al. (2013). Transcriptome analysis of *Cymbidium sinense* and its application to the identification of genes associated with floral development. *BMC Genomics* 14:279. doi: 10.1186/1471-2164-14-279
- Zhang, Y., De Stefano, R., Robine, M., Butelli, E., Bulling, K., Hill, L., et al. (2015). Different reactive oxygen species scavenging properties of flavonoids determine their abilities to extend the shelf life of tomato. *Plant Physiol.* 169, 1568–1583. doi: 10.1104/pp.15.00346

**Conflict of Interest Statement:** The authors declare that the research was conducted in the absence of any commercial or financial relationships that could be construed as a potential conflict of interest.

Copyright © 2017 Zhang, Zhao, Li, Zhang, Shi, Muhammad and Liang. This is an open-access article distributed under the terms of the Creative Commons Attribution License (CC BY). The use, distribution or reproduction in other forums is permitted, provided the original author(s) or licensor are credited and that the original publication in this journal is cited, in accordance with accepted academic practice. No use, distribution or reproduction is permitted which does not comply with these terms.